

Abstract

Both organic carbon (OC) and elemental carbon (EC) were measured at a rural site, Back Garden (BG), 50km northwest of the Guangzhou City, by using a semi-continuous thermal-optical analyzer during PRIDE-PRD 2006 summer intensive campaign. Together with the online EC/OC instrument, multiple instruments were also employed here which provided a good opportunity to check data quality. The regressions between the mass of organic aerosol (OM) and OC, as well as OC and water soluble organic carbon (WSOC) imply reliability of the data measured in this campaign. The average OC concentrations in fine particle for three typical periods during the campaign (local emission influence, typhoon and participation, normal days) were $28.1 \mu\text{g C m}^{-3}$, $4.0 \mu\text{g C m}^{-3}$ and $5.7 \mu\text{g C m}^{-3}$, respectively, and EC were $11.6 \mu\text{g C m}^{-3}$, $1.8 \mu\text{g C m}^{-3}$, and $3.3 \mu\text{g C m}^{-3}$ orderly. Diurnal variations of EC and OC showed that there were two peaks for EC and OC concentrations, i.e. at night and early morning, which were probably caused by the primary emission accumulation when the boundary layer was shallow. Compare to the constant diurnal enhancement ratios of primary EC, the enhancement ratio of OC (OC versus $(\text{CO}-\text{CO}_{\text{background}})$) remained in a relative high level in the afternoon with a similar diurnal variation to oxygenated organic aerosol (OOA), indicating the strong photochemical formation of OC. The traditional EC tracer method was modified to estimate the secondary organic carbon (SOC) formation, which shows that the average SOC concentration in BG site was about $2.0 \pm 2.3 \mu\text{g C m}^{-3}$. The SOC fraction in OC reached up to 80% with the average of 47%. Good correlations between estimated SOC versus measured OOA or WSOC, and estimated POC versus measured hydrocarbon-like organic aerosol (HOA) also proved the reliable results by the modified EC tracer method in this paper.

Carbonaceous aerosol at a rural site of PRD

W. W. Hu et al.

Title Page

Abstract

Introduction

Conclusions

References

Tables

Figures

◀

▶

◀

▶

Back

Close

Full Screen / Esc

Printer-friendly Version

Interactive Discussion



1 Introduction

Carbonaceous aerosol is the main constituent (20–80 % of fine particle) in the particulate matter (Lim and Turpin, 2002). Recently, carbonaceous aerosol has been one of the most hot research spots due to its important roles on climate and health effects, as well as its extreme complex properties (Ho et al., 2006). However, the classification of carbonaceous aerosol is still not clear due to the various detection methods (Lin et al., 2009). It is common to divide carbonaceous aerosol into two main fractions: organic carbon (OC) and element carbon (EC), which could be measured by the thermal/optical method. EC is emitted directly by primary combustion sources such as biomass burning (Andreae and Gelencser, 2006), vehicular exhaust (He et al., 2008), fossil combustion (Han et al., 2008). The OC is a poorly characterized aggregation of thousands of individual compounds from different sources (Seinfeld and Pandis, 1998). In general, the OC can be ascribed to primary organic carbon (POC) which is emitted by combustion sources similar to the EC sources or the primary biogenic sources, and secondary organic carbon (SOC) that is caused by the oxidation of volatile organic compounds (VOC) (Odum et al., 1997).

The state-of-art speciation techniques can identify only a small part of organic species in aerosol on molecular level. The influence of emission sources and atmospheric oxidation processes on carbonaceous aerosol is temporal which is on the time scale of minutes to hours (Schauer et al., 1996). Therefore high-time resolved estimation of the POC and SOC contributions become an important and useful way to understand the secondary organic formation process (Lim and Turpin, 2002). At present, one of the widely applied SOC estimation methods is the EC tracer method owing to its simplicity and reliance on ambient measurements alone (Turpin and Huntzicker, 1995; Cabada et al., 2004).

Pearl River Delta (PRD) region as the most developed city clusters is located in the southeast China and heavily influenced by the urban plumes (Cao et al., 2003). A few researches on carbonaceous aerosol in the PRD region were conducted, relative

Carbonaceous aerosol at a rural site of PRD

W. W. Hu et al.

Title Page

Abstract

Introduction

Conclusions

References

Tables

Figures



Back

Close

Full Screen / Esc

Printer-friendly Version

Interactive Discussion



high concentrations were detected, which were comparable to those in Beijing and Mexico City (Lin et al., 2009; Yu et al., 2009; Gnauk et al., 2008). However, most of the researches were filter based with low time resolution of 12 h/24 h (Cao et al., 2004; Duan et al., 2007; Ho et al., 2003), which can not reflect the dynamic revolution process of carbonaceous aerosol within one day. Therefore a higher time resolution research of carbonaceous aerosol in PRD region is needed to explore primary emission and secondary formation.

The Program of Regional Integrated Experiments of Air Quality over Pearl River Delta 2006 (PRIDE-PRD 2006) was conducted in July 2006, in which both EC and OC were measured by online Sunset EC/OC instrument from 3 July to 31 July. It was the first time that the hourly averaged time resolution concentrations of OC and EC in a rural site of PRD were detected, focused on twofold: (1) To find the carbonaceous aerosol characteristics in a rural site of PRD. (2) To distinguish and quantify the primary and secondary concentration of carbonaceous aerosol.

2 Experimental

2.1 Meteorology

The measurement was conducted at rural Back Garden, BG site (23.49° N, 113.03° E), about 50 km northwest to the Guangzhou City. The BG site was situated on the edge of the highly populated PRD region, though the area itself was mostly a farming area (Garland et al., 2008). The meteorology parameter was measured by Weather Transmitter (WXT510, Vaisala, Finland). In July 2006, the average temperature of the BG site was about $28.9 \pm 3.2^\circ\text{C}$ which is lower than Guangzhou by 1.6°C , relative humidity (RH) $78.0 \pm 13.7\%$ and ambient pressure $997 \pm 4\text{ hPa}$. The back trajectory clustering result by hysplit 4.9 model (<http://ready.arl.noaa.gov/hysplit-bin/trajtype.pl?runtype=archive>) showed that the wind direction of BG site is mainly from southeast or south (accounting for 81% of total wind). Thus, the BG site acts as a rural receptor for the

Carbonaceous aerosol at a rural site of PRD

W. W. Hu et al.

Title Page

Abstract

Introduction

Conclusions

References

Tables

Figures

◀

▶

◀

▶

Back

Close

Full Screen / Esc

Printer-friendly Version

Interactive Discussion



regional pollution resulting from the outflow of the heavily polluted city cluster around Guangzhou (Yue et al., 2010).

2.2 Measurement instruments

During PRIDE-PRD 2006 campaign, a number of instruments were used to measure aerosol and gas pollutants which can support us to do a comprehensive research on carbonaceous aerosols. The observation periods of different instruments are shown in Fig. 2 and brief descriptions of these instruments are given below.

The OC and EC concentrations in fine particle were measured hourly with an in situ semi-continuous OC and EC analyzer manufactured by Sunset Laboratory Inc. (Lin et al., 2009). The ambient aerosol was collected on a 1.03 cm² quartz filter through an 8 l min⁻¹ cyclone at the cut size of PM_{2.5} (from 3 July to 16 July) and PM₁ (from 17 July to 31 July), then analyzed by using improved NOISH 5040 temperature protocol. A denuder filled with carbon impregnated strip filters was setup to remove the artifacts of VOCs in front of the EC/OC instrument. The OC concentrations in this campaign were corrected by subtracting the remaining VOCs artifact from the measured OC concentrations which was around 2.0 μg C m⁻³ for PRD in general. More detailed description of Sunset OC and EC analyzer can be found in Lin et al. (2009). In this research, particle size distribution obtained by twin differential mobility particle size (TDMPS) shows the difference between PM_{2.5} and PM₁ was negligible (Yue et al., 2010). And also the mass concentrations of total water soluble organic compound (TWSOC), OC and OM/OC ratio in PM_{2.5} detected in the first half period campaign are similar to those in PM₁ in the second half period (Miyazaki et al., 2009). Therefore, the OC and EC data will be discussed without differentiating between PM_{2.5} and PM₁ in this paper.

The mass of organic aerosol (OM) and inorganic ions (sulfate, nitrate, ammonium and chloride) were measured by an aerosol mass spectrometry instrument (Q-AMS, Aerodyne Research Inc.). More specific descriptions of the instrument performance are given in the literatures (Takegawa et al., 2009; Xiao et al., 2009). The time resolution of AMS was 10 min and the adopted collection efficiency was 0.5. The accuracy

Carbonaceous aerosol at a rural site of PRD

W. W. Hu et al.

Title Page

Abstract

Introduction

Conclusions

References

Tables

Figures

◀

▶

◀

▶

Back

Close

Full Screen / Esc

Printer-friendly Version

Interactive Discussion



**Carbonaceous
aerosol at a rural site
of PRD**

W. W. Hu et al.

[Title Page](#)[Abstract](#)[Introduction](#)[Conclusions](#)[References](#)[Tables](#)[Figures](#)[⏪](#)[⏩](#)[◀](#)[▶](#)[Back](#)[Close](#)[Full Screen / Esc](#)[Printer-friendly Version](#)[Interactive Discussion](#)

of measurements was estimated to be 14 % based on the routine calibrations. The detection limits were 0.09, 0.03, 0.03, 0.5 and 0.4 $\mu\text{g m}^{-3}$ for SO_4^{2-} , NO_3^- , Cl^- , NH_4^+ and OM, respectively. The OM was divided into hydrocarbon-like organic aerosol (HOA) and oxygenated organic aerosol (OOA) by using positive matrix factorization (PMF) to mass spectrum.

Water soluble organic compound (WSOC) was measured by using a particle-into-liquid sampler (PILS). The details of the performance of PILS are given elsewhere (Miyazaki et al., 2009). The ambient aerosol was sampled at a flow rate of 16.7 l min^{-1} through a $\text{PM}_{2.5}$ cyclone. After particles were sampled, WSOC was quantified by an online total organic carbon (TOC) analyzer with the time resolution of 6 min and the detection limit of 0.1 $\mu\text{g m}^{-3}$.

Fine particle mass ($\text{PM}_{2.5}$) was measured by Tapered Element Oscillating Microbalance (TEOM) with half an hour time resolution.

The 24 h $\text{PM}_{2.5}$ sample were collected on the Teflon filters by using a four channel sampler (Anderson Inc.) with the flow rate of 8.3 l min^{-1} . After that water soluble ions including potassium ion (K^+) were analyzed by ion chromatography (ICS-90). The detection limits of K^+ was 0.1 $\mu\text{g m}^{-3}$.

The CO concentration was measured by Enhanced Trace Level CO Analyzer with an integration time of 1 min (48C-TLE-BCPAB, Thermo fisher company, USA). A Nafion dryer was used before the inlet of CO instrument to purify the sample air for avoiding the interference of water vapor. Zero calibrations were done every two hours. Meanwhile ozone (O_3) concentration was measured by UV absorption ozone analyzer (49C-B1NAB, Thermo Fisher Company), whose time resolution is 1 min as well. Zero calibration was performed at midnight of every day. Span calibrations on CO were done daily.

The boundary layer height was detected by Mini-MAX-DOAS. Details can be obtained in elsewhere (Li et al., 2010).

3 Results and discussion

3.1 Comparisons between organic aerosols

The OM concentration measured by the AMS and OC concentration measured by the Sunset EC/OC Analyzer within the whole campaign show a good correlation (R^2 is 0.86) in Fig. 3a. The fitting results of regression slope and intercept are 1.01 and 3.8, respectively. The slope is much lower than the result 1.88 reported in Takegawa et al. (2009), because we use the whole data set without getting rid of the high primary emission data as Takegawa et al. (2009) did. There are some OM data points below OC especially for the OC concentrations above $20 \mu\text{g C m}^{-3}$ due to the strong influence from the primary emissions.

The WSOC concentration measured by the PILS and OC concentration measured by the Sunset EC/OC Analyzer within the whole campaign show a good correlation (R^2 is 0.86) in Fig. 3b. The WSOC/OC ratio at BG site is about 50%, which is within the expected ranges, 20% to 80% (Kondo et al., 2007).

The comparisons among different carbonaceous aerosol shows Sunset OC results are believed reliable for the SOC data processing in the following.

3.2 The time series of carbonaceous aerosol

The time series of the mass concentrations for carbonaceous aerosol and the meteorological parameters are shown in Fig. 4. During the PRIDE-PRD 2006 campaign, the mass concentrations of carbonaceous aerosol in $\text{PM}_{2.5}$ varied dramatically. According to the source influence to carbonaceous aerosol and meteorology condition in the BG site, we define three typical days: normal days (grey bars), typhoon and participation days (white bars) and local emission influence days (black bar).

Local emission influence days (8% of total days): high concentrations of carbonaceous aerosol were measured from the noon of 23 to the midnight of 25 July, in average OC and EC were as high as $28.1 \pm 17.6 \mu\text{g C m}^{-3}$ and $11.6 \pm 15.1 \mu\text{g C m}^{-3}$, respectively (Table 1). Two obviously rapid increasing peaks of carbonaceous aerosol

Carbonaceous aerosol at a rural site of PRD

W. W. Hu et al.

Title Page

Abstract

Introduction

Conclusions

References

Tables

Figures

⏪

⏩

◀

▶

Back

Close

Full Screen / Esc

Printer-friendly Version

Interactive Discussion



**Carbonaceous
aerosol at a rural site
of PRD**

W. W. Hu et al.

Title Page

Abstract

Introduction

Conclusions

References

Tables

Figures

◀

▶

◀

▶

Back

Close

Full Screen / Esc

Printer-friendly Version

Interactive Discussion



with OC up to $82 \mu\text{g C m}^{-3}$ and EC up to $76 \mu\text{g C m}^{-3}$ were measured, while carbonaceous aerosol could explain about 50 % of the $\text{PM}_{2.5}$ increases. Meanwhile the OC/EC dropped sharply nearly to 1, which indicated that the increased OC was mainly due to local primary combustion sources. In addition, stagnant meteorological condition with the average wind speed below 1 m s^{-1} also facilitated the accumulation of aerosol concentrations.

To investigate the local emission sources in these two days, Cl^- and K^+ are checked which were obtained by the AMS instrument and daily four channel filter-IC analysis, respectively. The Cl^- can be an indicator for local primary emission sources, e.g. biomass burning, coal burning (Watson et al., 2001) and K^+ is usually used to indicate biomass burning (Andreae and Merlet, 2001). The Cl^- concentrations in local emission influence days increased rapidly from $0.8 \mu\text{g m}^{-3}$ (average concentration in the whole campaign) to $18.8 \mu\text{g m}^{-3}$. And the average K^+ concentration during these two days was $2.3 \mu\text{g m}^{-3}$ twice higher than the average concentration of whole campaign $1.1 \mu\text{g m}^{-3}$. Rapidly increased Cl^- and K^+ implied that the local emission possibly come from biomass burning around BG site. The indicator K^+/OC was about 0.1 implying the biomass burning in the BG site may come from agricultural residues burning (Andreae and Merlet, 2001).

Typhoon and precipitation days (27 % of total days): During the PRIDE-PRD 2006 campaign there were three participation processes of 10–11, 15–18, 26–27 July, and the last two precipitations were caused by the typhoons, Bilis and Kaemi (http://en.wikipedia.org/wiki/2006_Pacific_typhoon_season), respectively. Heavy rainfall and strong wind broke up the accumulation process of pollutants, and the OC and EC decreased with the average concentration of $4.0 \pm 2.8 \mu\text{g C m}^{-3}$ and $1.8 \pm 1.2 \mu\text{g C m}^{-3}$, respectively (Table 1).

Normal days (65 % of total days): the remaining observational days excluding the above two periods are defined to be normal days, which should reflect the usual ambient atmospheric condition. The OC and EC concentrations were $5.7 \pm 4.5 \mu\text{g C m}^{-3}$ and $3.3 \pm 2.8 \mu\text{g C m}^{-3}$, respectively (Table 1).

In the following discussion, in order to reflect normal carbonaceous aerosol status in the rural site of PRD, only normal days are focused on.

The concentrations of OC and EC in different cities are summarized in Table 2. Because of the upwind Guangzhou cities cluster influence (Yue et al., 2010), it is rationally found that the concentrations of OC and EC in the BG site were a little lower than that of Guangzhou at the same period. OC and EC concentration levels in both Guangzhou urban and BG rural sites of the PRD region were comparable with those in the Mexico region which is one of the biggest mega cities in the world (Aiken et al., 2009; Yu et al., 2009; Verma et al., 2010). The other downwind rural sites (Ho et al., 2006; Polidori et al., 2006; Viana et al., 2007) are also listed in the Table 2 and found that during the summer time the carbonaceous concentration in PRD is higher than the other rural sites, especially for the EC.

3.3 Diurnal profile of carbonaceous aerosol

Pronounced diurnal variations were observed for primary species EC and CO, showed in Fig. 5a and c. The EC diurnal profile varied by a factor 4 with high peak at night and low valley in the afternoon. The EC concentrations kept high levels during the night and early morning, which was probably due to the accumulation of direct night time emissions and the remains of shallow boundary layer, the EC peaks reached at 4.6 (02:00) and $4.7 \mu\text{g C m}^{-3}$ (06:00), respectively. After sunrise at 09:00, the observed EC dropped sharply due to the quick expanding boundary layer and attendant increased wind speed. The lowest average EC concentration was observed in the afternoon $1.2 \mu\text{g C m}^{-3}$ at 14:00. And then after 16:00 the boundary layer height started to decrease, consequently the observed EC concentration increased again. The diurnal profile of CO has very similar variation with that of EC, indicating the same emission sources of both. The diurnal profile of OC was similar to that of EC, varied by a factor about 2 (Fig. 5b). However, there is no obviously decreasing of OC during the day which may caused by the secondary organic formation. The maximum peak around 02:00, $8.0 \mu\text{g C m}^{-3}$ and second peak around 07:00, $6.8 \mu\text{g C m}^{-3}$.

Carbonaceous aerosol at a rural site of PRD

W. W. Hu et al.

Title Page

Abstract

Introduction

Conclusions

References

Tables

Figures

◀

▶

◀

▶

Back

Close

Full Screen / Esc

Printer-friendly Version

Interactive Discussion



**Carbonaceous
aerosol at a rural site
of PRD**

W. W. Hu et al.

Title Page

Abstract

Introduction

Conclusions

References

Tables

Figures

⏪

⏩

◀

▶

Back

Close

Full Screen / Esc

Printer-friendly Version

Interactive Discussion



In order to evaluate the secondary formation of organic aerosol, CO as an inertia combustion tracer is adopted here to exclude the influence on emissions and transport for a certain extent by normalizing the OC and EC (de Gouw et al., 2009). The diurnal profiles of different aerosol species versus ($\text{CO}-\text{CO}_{\text{Background}}$) are done in Fig. 6. The background concentration of CO is calculated as the lowest 5 percentile of the CO mixing ratios observed during the normal days of campaign, 0.16 ppm (Miyazaki et al., 2009).

In the Fig. 6a, the ratio of $\text{EC}/(\text{CO}-0.16)$ is scaled from 2.5 to $12.5 \mu\text{g m}^{-3} \text{ppm}^{-1}$, with the average of $7.9 \mu\text{g m}^{-3} \text{ppm}^{-1}$. The profile of enhancement ratio of EC is relative constant, indicating the similar profiles between EC and CO emission sources. The EC profile here is also similar to the result in Mexico suburb T1 site which also keep relative constant diurnal profile across the whole day (de Gouw et al., 2009).

The OOA measured by the AMS is believed typical secondary production. The diurnal variation of OOA shows clearly variations with an extreme high enhancement ratio in the afternoon indicating the strong secondary formation. OC and OM enhancement ratios display very similar to that of OOA, implying secondary formations plays an important role in both OC and OM. The profiles of OC enhancement ratio between BG and northeast coastal city of US are very similar, Fig. 6b. However, the OM enhancement ratio in BG as showed in Fig. 6c is much higher that of the urban plumes in the US (de Gouw et al., 2009). The difference between OC and OM comparison is probably caused by the other chemical compositions in the OM. On the whole, the contributions of secondary formation to OC or OM were obviously observed, especially in the afternoon when the photochemical activity was strong. Yue et al. (2010) also found the secondary transformation occurred and played an important role during regional transport in PRD region. Thus, to investigate secondary organic formation, the quantification of secondary organic carbon process was examined in the following.

3.4 Estimation of secondary organic carbon by modified EC tracer method

EC tracer method is usually adopted to estimate the SOC concentration. The EC tracer method assumes EC is a tracer of primary emission. Since the primary OC and EC almost come from the same combustion sources, through calculating the emission ratio of primary OC to EC, we can calculate the POC concentration and then SOC (POC + SOC = OC). So the determination $(OC/EC)_{pri}$ is the key factor in the EC tracer method.

In previous studies, the $(OC/EC)_{pri}$ has been estimated on the basis of two methods. (1) Ambient OC and EC concentrations at locations is influenced mainly from primary source emissions and the secondary organic aerosol formation is expected to be low (Turpin and Huntzicker, 1995). However it is really hard to draw a clear distinction between primary source dominant period and secondary source dominant period. (2) Primary emission inventories of OC and EC (Gray et al., 1986). Although the primary emission inventories of OC and EC are used widely, if the primary sources are complicated, the uncertainty of $(OC/EC)_{pri}$ derived from primary emission inventories will be very large, especially under the complicated condition of China (Cabada et al., 2004; Millet et al., 2005).

To improve the accuracy of SOC estimation, modification on traditional EC tracer method is done here to obtain a more specific $(OC/EC)_{pri}$. That is to combine traditional EC tracer method with source tracer ratio method which is firstly introduced by Millet et al. (2005). The good agreement of source tracer ratio method has been confirmed in Zhang et al. (2005). Detailed description about source tracer ratio method can be obtained in the Millet et al. (2005). The modified EC tracer method is explained below. An unraveled OC equation was given by:

$$OC_{total} = OC_{pri} + OC_{sec} + OC_{non} = EC_a \times (OC/EC)_{pri} + OC_{sec} + OC_{non} \quad (1)$$

$$OC_{sec} = OC_{total} - EC_a \times (OC/EC)_{pri} - OC_{non} \quad (2)$$

Carbonaceous aerosol at a rural site of PRD

W. W. Hu et al.

Title Page

Abstract

Introduction

Conclusions

References

Tables

Figures

⏪

⏩

◀

▶

Back

Close

Full Screen / Esc

Printer-friendly Version

Interactive Discussion



Here, OC_{total} is the measured OC concentrations, which could be separated into two parts: primary organic carbon (OC_{pri}) and secondary formation organic carbon (OC_{sec}), as well as a regional background (OC_{other}). $(OC/EC)_{pri}$ is the initially emission ratio between OC_{pri} and EC from combustion source. EC_a represents the real ambient observed EC concentration.

OC_{non} is the non-combustion OC which may come from biogenic primary OC or regional OC background. OC_{non} is suggested to be small and it will not significantly affect our results, Here, we prefer not to consider OC_{non} in this study, which is consistent with the former studies (Lim and Turpin, 2002; Cabada et al., 2004; Polidori et al., 2006). So the equation can be simplified to Eq. (3).

$$OC_{sec} = OC_{total} - EC_a \times (OC/EC)_{pri} \quad (3)$$

In Eq. (3) only OC_{sec} and $(OC/EC)_{pri}$ are unknown. So to calculate OC_{sec} concentration, the key is to find an exact $(OC/EC)_{pri}$. In the modified EC tracer method, the first step is to find a proper period dataset to calculate $(OC/EC)_{pri}$. From the diurnal variation of carbonaceous aerosol, it is found that the sources of carbonaceous aerosol are different between day and night. So the $(OC/EC)_{pri}$ calculation will be separated into two datasets: OC and EC in day (06:00–18:00) and in night (18:00–06:00). Then, the second step is to calculate $(OC/EC)_{pri}$ using one of the OC and EC dataset. From the Eq. (3), when $(OC/EC)_{pri}$ is given a fixed reasonable value, OC_{sec} and the coefficient of determination (R^2) between OC_{sec} and EC within one dataset could be correspondingly determined. By varying $(OC/EC)_{pri}$ value in a rational range (0–15 is used here with a step of 0.001), a series of R^2 between OC_{sec} and EC in one dataset can be obtained. A plot of the R^2 between OC_{sec} and EC via $(OC/EC)_{pri}$ value can be drawn. Since the OC_{sec} and EC were totally from different sources, the proper $(OC/EC)_{pri}$ should be the one that corresponds to the minimum R^2 value meaning that OC_{sec} worst correlated with EC. Then the day or night $(OC/EC)_{pri}$ can be determined within the whole campaign.

Carbonaceous aerosol at a rural site of PRD

W. W. Hu et al.

Title Page

Abstract

Introduction

Conclusions

References

Tables

Figures

⏪

⏩

◀

▶

Back

Close

Full Screen / Esc

Printer-friendly Version

Interactive Discussion



**Carbonaceous
aerosol at a rural site
of PRD**

W. W. Hu et al.

Title Page

Abstract

Introduction

Conclusions

References

Tables

Figures

⏪

⏩

◀

▶

Back

Close

Full Screen / Esc

Printer-friendly Version

Interactive Discussion



In order to check the reliability of modified EC tracer method, $(OC/EC)_{pri}$ in local emission influence days is also calculated as an example, Fig. 7a. From 23 to 25, there are very strong primary emissions at night, which has been discussed in Sect. 3.1. Highly relevant linear relationship between OC and EC also indicated that the OC was mainly dominated by primary sources. The regression slope between OC and EC shows the $(OC/EC)_{pri}$ is 1.06. Meanwhile the $(OC/EC)_{pri}$ by modified EC tracer method is 1.04. The agreement between regression result and modified EC tracer method indicated the proper and reasonableness of the latter method.

The SOC concentrations are calculated by the estimation of $(OC/EC)_{pri}$ of 1.57 and 1.42 for the day and night of normal days, respectively, Fig. 7c. Overall, the SOC concentration can be up to $15.6 \mu\text{g m}^{-3}$ with the average concentration of $2.0 \pm 2.3 \mu\text{g m}^{-3}$. The SOC fraction in OC is ranged up to 80% with the average of 47% (Fig. 8a). The concentrations of WSOC correlate well with the R^2 0.7 and regression slope 0.7 ± 0.03 , indicating most of WSOC are mainly SOC. The R^2 between SOC and OOA is fine that is about 0.6. The regression slope between them is 0.31, a little lower than the result in Pittsburgh ~ 0.45 (Zhang et al., 2005), which may be caused by the differential of non-carbon fraction in OOA. However the HOA correlated POC very well. The R^2 between POC and HOA is about 0.76. And the regression slope between POC and HOA is about 0.9 indicating that most or all HOA is POC. The POC and HOA ratio is similar to result ~ 0.8 in Mexico city T0 site (Aiken et al., 2009) and ~ 0.8 in Pittsburgh as well (Zhang et al., 2005).

It is noticed that strong secondary formation episode happened from 19 to 21 July during the whole campaign with the enhancement of strong solar radiation and weak wind. Therefore this episode is used to evaluate the estimation of the secondary formation at the BG site (Fig. 9). The ratio of SOC to OC showed a distinctive diurnal profile with highest ratio in the afternoon and lowest at night, matching well with the profiles of O_3 concentrations. The average SOC in the afternoon from 14:00 to 17:00 accounted for 64% of OC within these three days.

4 Conclusions

Carbonaceous aerosol was measured at Back Garden, a rural site of the PRD region during PRIDE-PRD 2006 campaign in July 2006. It is found that the concentrations of carbonaceous aerosol could vary dramatically due to the extremely meteorology conditions (e.g. typhoon and precipitation) and anthropogenic emission sources (e.g. biomass burning) in the summer of PRD.

The similar diurnal profiles for OC and EC were observed with two peaks at night and early morning owing to the local emissions accumulation in shallow boundary layer and rush hour emission in the early morning, minimum in the afternoon due to the dilution effect by the lifted boundary layer. The enhancement ratio of OC shows similar diurnal variation to oxygenated organic aerosol (OOA) with a relative high peak in the afternoon indicating the strong photochemical secondary formation.

The modified EC tracer method was adopted to estimation of secondary organic carbon (SOC) formation. According to the diurnal characteristic of carbonaceous aerosols, the key factor of $(OC/EC)_{pri}$ was calculated by the day and night, respectively. It is found that average SOC concentration at the BG site is $2.0 \pm 2.3 \mu\text{g C m}^{-3}$, accounted for 47 % of the OC mass concentration, and can be up to 80 % periodically. Good correlation between estimated SOC versus measured OOA or WSOC, and estimated POC versus measured HOA are also proved the reliable results by the modified EC tracer method in this paper.

Acknowledgements. This work is supported by the National Natural Science Foundation of China (20977001,21025728), and also supported by the China Ministry of Environmental Protection's Special Funds for Scientific Research on Public Welfare (201009002) and EU FP-7 CityZen project (212095). We would like sincerely thank the PRIDE-PRD 2006 team.

ACPD

11, 21601–21629, 2011

Carbonaceous aerosol at a rural site of PRD

W. W. Hu et al.

Title Page

Abstract

Introduction

Conclusions

References

Tables

Figures

⏪

⏩

◀

▶

Back

Close

Full Screen / Esc

Printer-friendly Version

Interactive Discussion



References

- Aiken, A. C., Salcedo, D., Cubison, M. J., Huffman, J. A., DeCarlo, P. F., Ulbrich, I. M., Docherty, K. S., Sueper, D., Kimmel, J. R., Worsnop, D. R., Trimborn, A., Northway, M., Stone, E. A., Schauer, J. J., Volkamer, R. M., Fortner, E., de Foy, B., Wang, J., Laskin, A., Shuttanandan, V., Zheng, J., Zhang, R., Gaffney, J., Marley, N. A., Paredes-Miranda, G., Arnott, W. P., Molina, L. T., Sosa, G., and Jimenez, J. L.: Mexico City aerosol analysis during MILAGRO using high resolution aerosol mass spectrometry at the urban supersite (T0) – Part 1: Fine particle composition and organic source apportionment, *Atmos. Chem. Phys.*, 9, 6633–6653, doi:10.5194/acp-9-6633-2009, 2009.
- Andreae, M. O. and Gelencsér, A.: Black carbon or brown carbon? The nature of light-absorbing carbonaceous aerosols, *Atmos. Chem. Phys.*, 6, 3131–3148, doi:10.5194/acp-6-3131-2006, 2006.
- Andreae, M. O. and Merlet, P.: Emission of trace gases and aerosols from biomass burning, *Global Biogeochem. Cycles*, 15, 955–966, 2001.
- Cabada, J. C., Pandis, S. N., Subramanian, R., Robinson, A. L., Polidori, A., and Turpin, B.: Estimating the secondary organic aerosol contribution to PM_{2.5} using the EC tracer method, *Aerosol Sci. Technol.*, 38, 140–155, doi:10.1080/02786820390229084, 2004.
- Cao, J. J., Lee, S. C., Ho, K. F., Zhang, X. Y., Zou, S. C., Fung, K., Chow, J. C., and Watson, J. G.: Characteristics of carbonaceous aerosol in Pearl River Delta Region, China during 2001 winter period, *Atmos. Environ.*, 37, 1451–1460, doi:10.1016/S1352-2310(02)01002-6, 2003.
- de Gouw, J. A., Welsh-Bon, D., Warneke, C., Kuster, W. C., Alexander, L., Baker, A. K., Beyersdorf, A. J., Blake, D. R., Canagaratna, M., Celada, A. T., Huey, L. G., Junkermann, W., Onasch, T. B., Salcido, A., Sjostedt, S. J., Sullivan, A. P., Tanner, D. J., Vargas, O., Weber, R. J., Worsnop, D. R., Yu, X. Y., and Zaveri, R.: Emission and chemistry of organic carbon in the gas and aerosol phase at a sub-urban site near Mexico City in March 2006 during the MILAGRO study, *Atmos. Chem. Phys.*, 9, 3425–3442, doi:10.5194/acp-9-3425-2009, 2009.
- Garland, R. M., Yang, H., Schmid, O., Rose, D., Nowak, A., Achtert, P., Wiedensohler, A., Takegawa, N., Kita, K., Miyazaki, Y., Kondo, Y., Hu, M., Shao, M., Zeng, L. M., Zhang, Y. H., Andreae, M. O., and Pöschl, U.: Aerosol optical properties in a rural environment near the mega-city Guangzhou, China: implications for regional air pollution, radiative forcing and remote sensing, *Atmos. Chem. Phys.*, 8, 5161–5186, doi:10.5194/acp-8-5161-2008, 2008.

Carbonaceous aerosol at a rural site of PRD

W. W. Hu et al.

Title Page

Abstract

Introduction

Conclusions

References

Tables

Figures

◀

▶

◀

▶

Back

Close

Full Screen / Esc

Printer-friendly Version

Interactive Discussion



**Carbonaceous
aerosol at a rural site
of PRD**

W. W. Hu et al.

Title Page

Abstract

Introduction

Conclusions

References

Tables

Figures

◀

▶

◀

▶

Back

Close

Full Screen / Esc

Printer-friendly Version

Interactive Discussion



Gnauk, T., Müller, K., van Pinxteren, D., He, L.-Y., Niu, Y., Hu, M., and Herrmann, H.: Size-segregated particulate chemical composition in Xinken, Pearl River Delta, China: OC/EC and organic compounds, *Atmos. Environ.*, 42, 6296–6309, doi:10.1016/j.atmosenv.2008.05.001, 2008.

5 Gray, H. A., Cass, G. R., Huntzicker, J. J., Heyerdahl, E. K., and Rau, J. A.: Characteristics of Atmospheric Organic and Elemental Carbon Particle Concentrations in Los-Angeles, *Environ. Sci. Technol.*, 20, 580–589, 1986.

Han, Y. M., Han, Z. W., Cao, J. J., Chow, J. C., Watson, J. G., An, Z. S., Liu, S. X., and Zhang, R. J.: Distribution and origin of carbonaceous aerosol over a rural high-mountain
10 lake area, Northern China and its transport significance, *Atmos. Environ.*, 42, 2405–2414, doi:10.1016/j.atmosenv.2007.12.020, 2008.

He, L. Y., Hu, M., Zhang, Y. H., Huang, X. F., and Yao, T. T.: Fine particle emissions from on-road vehicles in the Zhujiang Tunnel, China, *Environ. Sci. Technol.*, 42, 4461–4466, doi:10.1021/Es7022658, 2008.

15 Ho, K. F., Lee, S. C., Cao, J. J., Li, Y. S., Chow, J. C., Watson, J. G., and Fung, K.: Variability of organic and elemental carbon, water soluble organic carbon, and isotopes in Hong Kong, *Atmos. Chem. Phys.*, 6, 4569–4576, doi:10.5194/acp-6-4569-2006, 2006.

Kondo, Y., Miyazaki, Y., Takegawa, N., Miyakawa, T., Weber, R. J., Jimenez, J. L., Zhang, Q., and Worsnop, D. R.: Oxygenated and water-soluble organic aerosols in Tokyo, *J. Geophys. Res.-Atmos.*, 112, D01203, doi:10.1029/2006JD007056, 2007.

20 Li, X., Brauers, T., Shao, M., Garland, R. M., Wagner, T., Deutschmann, T., and Wahner, A.: MAX-DOAS measurements in southern China: retrieval of aerosol extinctions and validation using ground-based in-situ data, *Atmos. Chem. Phys.*, 10, 2079–2089, doi:10.5194/acp-10-2079-2010, 2010.

25 Lim, H. J. and Turpin, B. J.: Origins of primary and secondary organic aerosol in Atlanta: Results of time-resolved measurements during the Atlanta supersite experiment, *Environ. Sci. Technol.*, 36, 4489–4496, doi:10.1021/Es0206487, 2002.

Lin, P., Hu, M., Deng, Z., Slanina, J., Han, S., Kondo, Y., Takegawa, N., Miyazaki, Y., Zhao, Y., and Sugimoto, N.: Seasonal and diurnal variations of organic carbon in PM_{2.5} in Beijing and the estimation of secondary organic carbon, *J. Geophys. Res.-Atmos.*, 114, D00G11, doi:10.1029/2008JD010902, 2009.

30 Millet, D. B., Donahue, N. M., Pandis, S. N., Polidori, A., Stanier, C. O., Turpin, B. J., and Goldstein, A. H.: Atmospheric volatile organic compound measurements during the Pitts-

**Carbonaceous
aerosol at a rural site
of PRD**

W. W. Hu et al.

Title Page

Abstract

Introduction

Conclusions

References

Tables

Figures

◀

▶

◀

▶

Back

Close

Full Screen / Esc

Printer-friendly Version

Interactive Discussion



burgh Air Quality Study: Results, interpretation, and quantification of primary and secondary contributions, *J. Geophys. Res.-Atmos.*, 110, D07S07, doi:10.1029/2004jd004601, 2005.

Miyazaki, Y., Kondo, Y., Shiraiwa, M., Takegawa, N., Miyakawa, T., Han, S., Kita, K., Hu, M., Deng, Z. Q., Zhao, Y., Sugimoto, N., Blake, D. R., and Weber, R. J.: Chemical characteriza-
5 tion of water-soluble organic carbon aerosols at a rural site in the Pearl River Delta, China, in the summer of 2006, *J. Geophys. Res.-Atmos.*, 114, D14208, doi:10.1029/2009jd011736, 2009.

Odum, J. R., Jungkamp, T. P. W., Griffin, R. J., Flagan, R. C., and Seinfeld, J. H.: The atmospheric aerosol-forming potential of whole gasoline vapor, *Science*, 276, 96–99, 1997.

10 Park, S. S., Harrison, D., Pancras, J. P., and Ondov, J. M.: Highly time-resolved organic and elemental carbon measurements at the Baltimore Supersite in 2002, *J. Geophys. Res.-Atmos.*, 110, D07S06, doi:10.1029/2004jd004610, 2005.

Polidori, A., Turpin, B. J., Lim, H. J., Cabada, J. C., Subramanian, R., Pandis, S. N., and Robinson, A. L.: Local and regional secondary organic aerosol: Insights from a year of
15 semi-continuous carbon measurements at Pittsburgh, *Aerosol Sci. Technol.*, 40, 861–872, doi:10.1080/02786820600754649, 2006.

Schauer, J. J., Rogge, W. F., Hildemann, L. M., Mazurek, M. A., and Cass, G. R.: Source apportionment of airborne particulate matter using organic compounds as tracers, *Atmos. Environ.*, 30, 3837–3855, 1996.

20 Seinfeld, J. H. and Pandis, S. N.: *Atmospheric Chemistry and Physics: from Air Pollution to Climate Change*, John Wiley, New York, 1998.

Takegawa, N., Miyakawa, T., Watanabe, M., Kondo, Y., Miyazaki, Y., Han, S., Zhao, Y., van Pinxteren, D., Brüggemann, E., Gnauk, T., Herrmann, H., Xiao, R., Deng, Z., Hu, M., Zhu, T., and Zhang, Y.: Performance of an Aerodyne Aerosol Mass Spectrometer (AMS) during
25 Intensive Campaigns in China in the Summer of 2006, *Aerosol Sci. Technol.*, 43, 189–204, doi:10.1080/02786820802582251, 2009.

Tao, J., Ho, K. F., Chen, L. G., Zhu, L. H., Han, J. L., and Xu, Z. C.: Effect of chemical composition of PM_{2.5} on visibility in Guangzhou, China, 2007 spring, *Particuology*, 7, 68–75, doi:10.1016/j.partic.2008.11.002, 2009.

30 Turpin, B. J. and Huntzicker, J. J.: Identification of Secondary Organic Aerosol Episodes and Quantitation of Primary and Secondary Organic Aerosol Concentrations during Scaqs, *Atmos. Environ.*, 29, 3527–3544, 1995.

Verma, R. L., Sahu, L. K., Kondo, Y., Takegawa, N., Han, S., Jung, J. S., Kim, Y. J., Fan,

**Carbonaceous
aerosol at a rural site
of PRD**

W. W. Hu et al.

[Title Page](#)[Abstract](#)[Introduction](#)[Conclusions](#)[References](#)[Tables](#)[Figures](#)[⏪](#)[⏩](#)[◀](#)[▶](#)[Back](#)[Close](#)[Full Screen / Esc](#)[Printer-friendly Version](#)[Interactive Discussion](#)

S., Sugimoto, N., Shammaa, M. H., Zhang, Y. H., and Zhao, Y.: Temporal variations of black carbon in Guangzhou, China, in summer 2006, *Atmos. Chem. Phys.*, 10, 6471–6485, doi:10.5194/acp-10-6471-2010, 2010.

5 Viana, M., Maenhaut, W., ten Brink, H. M., Chi, X., Weijers, E., Querol, X., Alastuey, A., Mikuska, P., and Vecera, Z.: Comparative analysis of organic and elemental carbon concentrations in carbonaceous aerosols in three European cities, *Atmos. Environ.*, 41, 5972–5983, doi:10.1016/j.atmosenv.2007.03.035, 2007.

10 Watson, J. G., Chow, J. C., and Houck, J. E.: PM_{2.5} chemical source profiles for vehicle exhaust, vegetative burning, geological material, and coal burning in Northwestern Colorado during 1995, *Chemosphere*, 43, 1141–1151, doi:10.1016/s0045-6535(00)00171-5, 2001.

Xiao, R., Takegawa, N., Kondo, Y., Miyazaki, Y., Miyakawa, T., Hu, M., Shao, M., Zeng, L. M., Hofzumahaus, A., Holland, F., Lu, K., Sugimoto, N., Zhao, Y., and Zhang, Y. H.: Formation of submicron sulfate and organic aerosols in the outflow from the urban region of the Pearl River Delta in China, *Atmos. Environ.*, 43, 3754–3763, doi:10.1016/j.atmosenv.2009.04.028, 2009.

15 Yu, X.-Y., Cary, R. A., and Laulainen, N. S.: Primary and secondary organic carbon downwind of Mexico City, *Atmos. Chem. Phys.*, 9, 6793–6814, doi:10.5194/acp-9-6793-2009, 2009.

20 Yue, D. L., Hu, M., Wu, Z. J., Guo, S., Wen, M. T., Nowak, A., Wehner, B., Wiedensohler, A., Takegawa, N., Kondo, Y., Wang, X. S., Li, Y. P., Zeng, L. M., and Zhang, Y. H.: Variation of particle number size distributions and chemical compositions at the urban and downwind regional sites in the Pearl River Delta during summertime pollution episodes, *Atmos. Chem. Phys.*, 10, 9431–9439, doi:10.5194/acp-10-9431-2010, 2010.

25 Zhang, Q., Worsnop, D. R., Canagaratna, M. R., and Jimenez, J. L.: Hydrocarbon-like and oxygenated organic aerosols in Pittsburgh: insights into sources and processes of organic aerosols, *Atmos. Chem. Phys.*, 5, 3289–3311, doi:10.5194/acp-5-3289-2005, 2005.

Carbonaceous aerosol at a rural site of PRD

W. W. Hu et al.

Table 1. Comparisons of carbonaceous aerosol concentrations in three typical periods in the PRIDE-PRD 2006 campaign.

Classification of measurement period (time periods)		OC ($\mu\text{g C m}^{-3}$)	EC ($\mu\text{g C m}^{-3}$)	TC*/PM _{2.5} (%)
Typhoon and precipitation days	10–11, 15–18, 26–27 Jul 2006	4.0±2.8	1.8±1.2	12.5
Local emission influence days	23–25 Jul 2006	28.1±17.6	11.6±15.1	18.2
Normal days	except the two periods above	5.7±4.5	3.3±2.8	10.1
Total in average		7.6±5.7	3.7±5.7	13.6

* TC = OC + EC

Title Page

Abstract

Introduction

Conclusions

References

Tables

Figures

◀

▶

◀

▶

Back

Close

Full Screen / Esc

Printer-friendly Version

Interactive Discussion



Carbonaceous aerosol at a rural site of PRD

W. W. Hu et al.

Title Page

Abstract

Introduction

Conclusions

References

Tables

Figures

◀

▶

◀

▶

Back

Close

Full Screen / Esc

Printer-friendly Version

Interactive Discussion



Table 2. Comparisons of carbonaceous aerosol concentration with other studies in China and other countries.

Location	Station types and mayor source	Period	Analysis method	OC ($\mu\text{g C m}^{-3}$)	EC ($\mu\text{g C m}^{-3}$)	Reference
BG, China	Regional site; Downwind of the Urban (Normal days)	Jul 2006 (normal day)	TOT	5.7	3.3	This study
Guangzhou, China	Urban site; Vehicle, industrial, domestic activities	Jul 2006	TOT	8.9	4.7	Verma et al. (2010)
Guangzhou, China	Urban site	Apr 2007	TOR	14.8	8.1	Tao et al. (2009)
Beijing, China	Urban site	Summer 2006	TOT	10.0	2.2	Lin et al. (2009)
Hong Kong, China	Regional site	Summer 2006	TOR	1.5	0.4	Ho et al. (2006)
Gwangju, Korea	Urban site; motor vehicle emission	Mar–May 2001	TOT	15.7	5.7	Park et al. (2005)
T0, Mexico ^a	Urban site	Mar 2006	TOR	Nan	4.2	Aiken et al. (2009)
T1, Mexico ^b	Suburb site; Downwind of the urban	Mar 2006	TOT	6.4	2.1	Yu et al. (2009)
T2, Mexico ^c	Non-urban site; Downwind of the urban	Mar 2006	TOT	5.4	0.6	Yu et al. (2009)
Pittsburgh, USA	Regional site; No local emissions	Jul 2001–Aug 2002	TOT	2.75	0.89	Polidori et al. (2006)
Barcelona, Spain	Urban background site; influenced by traffic emission transportation	Summer 2004	TOT	3.6	1.5	Viana et al. (2007)

^a T0 site was an urban site located in the center of Mexico City.

^b T1 site was a suburb site in the down wind direction of Mexico City.

^c T2 site was a regional background site of Mexico City.

TOT: thermal/optical transmission. TOR: thermal/optical reflectance.

Carbonaceous aerosol at a rural site of PRD

W. W. Hu et al.

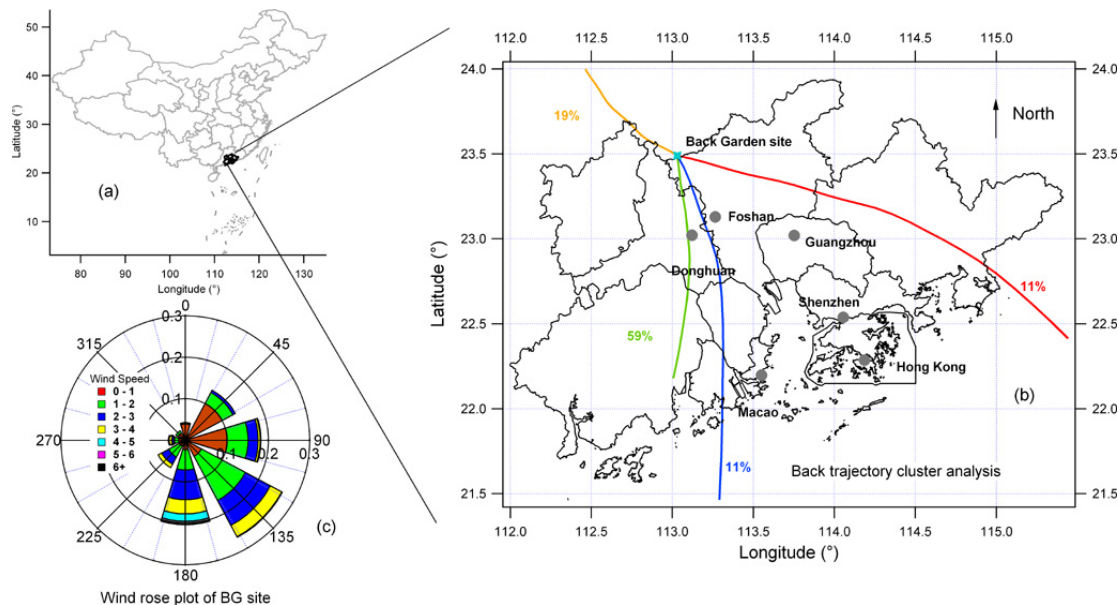


Fig. 1. (a) Map of the PRD area in China. (b) Location of Back Garden site (BG) and major cities related in this study, and also showed the back trajectory cluster analysis results. (c) wind rose plot of BG site in July 2006.

[Title Page](#)
[Abstract](#)
[Introduction](#)
[Conclusions](#)
[References](#)
[Tables](#)
[Figures](#)
[Back](#)
[Close](#)
[Full Screen / Esc](#)
[Printer-friendly Version](#)
[Interactive Discussion](#)

Carbonaceous aerosol at a rural site of PRD

W. W. Hu et al.

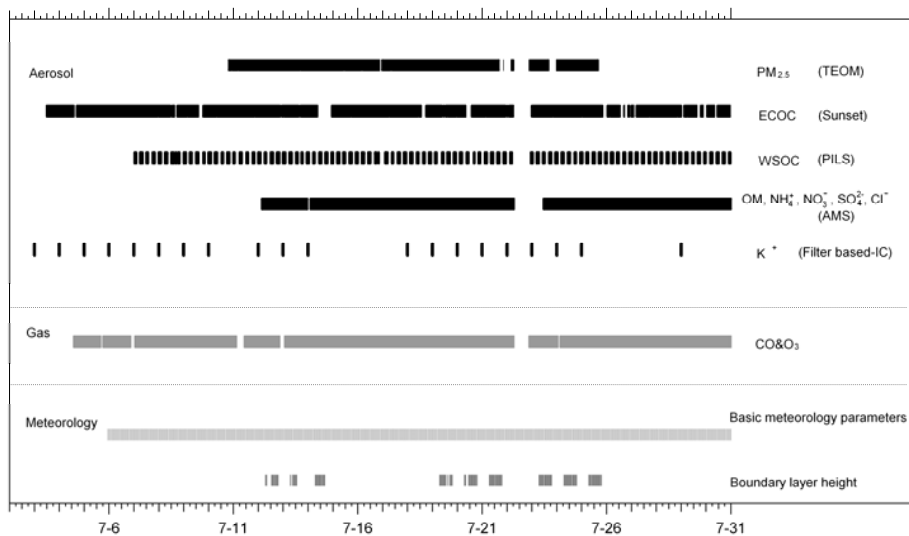


Fig. 2. The instruments used to measure aerosol and gas species at the BG site in PRIDE-PRD 2006 campaign.

Carbonaceous aerosol at a rural site of PRD

W. W. Hu et al.

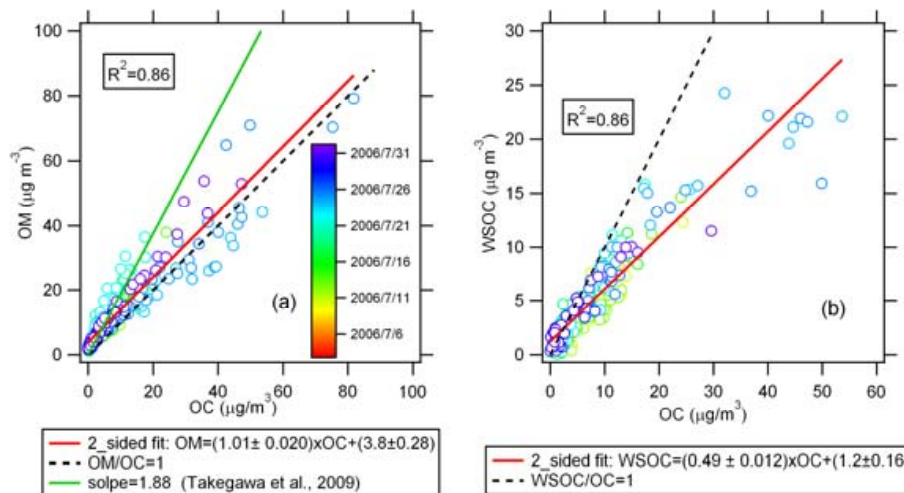


Fig. 3. The comparisons of measured data between **(a)** OM and OC; **(b)** WSOC and OC.

Title Page

Abstract

Introduction

Conclusions

References

Tables

Figures

◀

▶

◀

▶

Back

Close

Full Screen / Esc

Printer-friendly Version

Interactive Discussion



Carbonaceous aerosol at a rural site of PRD

W. W. Hu et al.

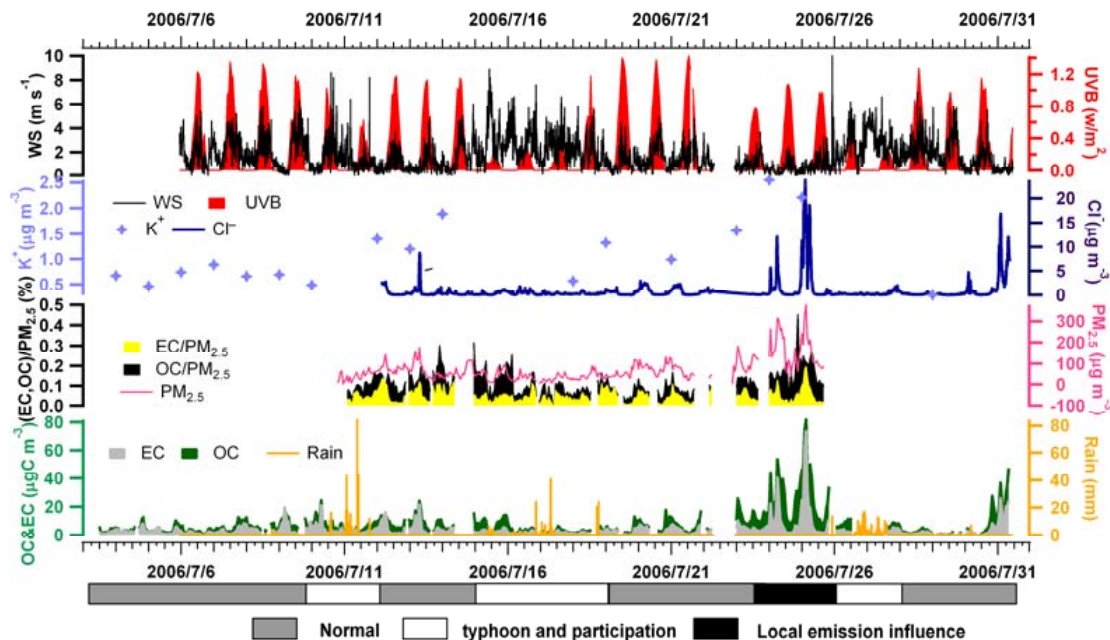


Fig. 4. The time series mass concentrations of $\text{PM}_{2.5}$, EC, OC, Cl^- , K^+ and meteorology conditions during PRIDE-PRD 2006 campaign. The whole campaign was divided into three typical periods: normal days (grey bar), typhoon and precipitation days (white bar) and local emission influence days (black bar).

Title Page

Abstract

Introduction

Conclusions

References

Tables

Figures

◀

▶

◀

▶

Back

Close

Full Screen / Esc

Printer-friendly Version

Interactive Discussion



**Carbonaceous
aerosol at a rural site
of PRD**

W. W. Hu et al.

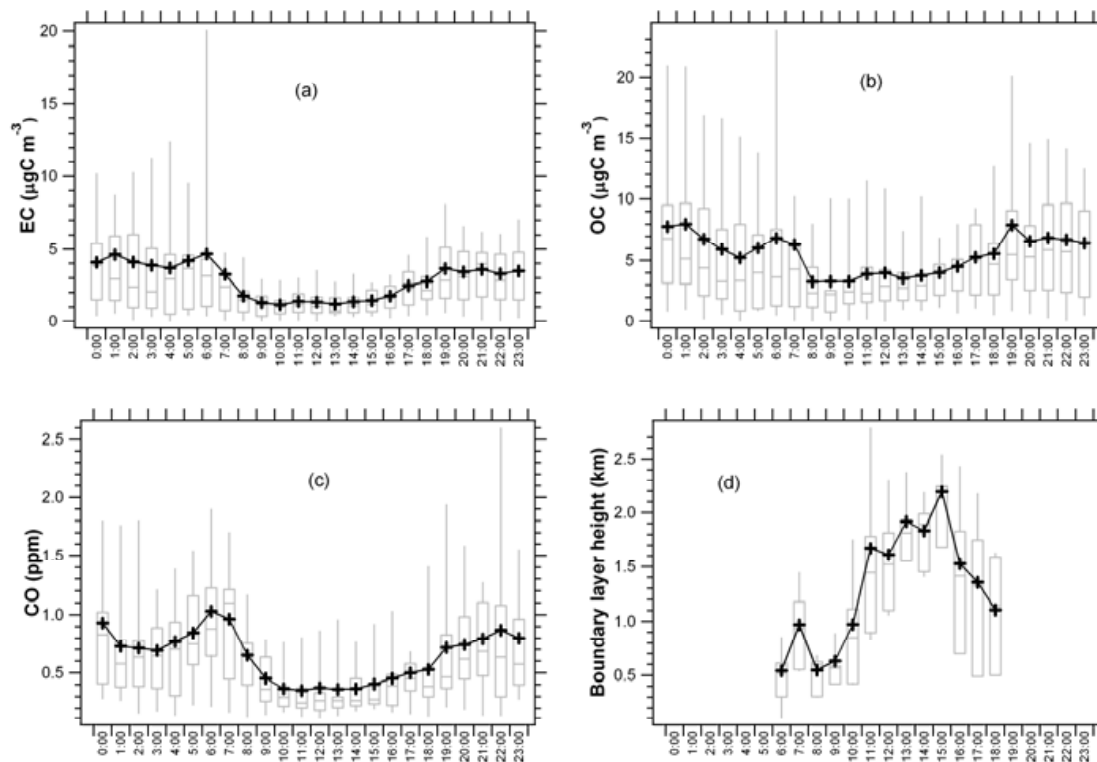


Fig. 5. Diurnal variation box plots of EC (a), OC (b), CO (c), and boundary layer height (d). The upper and lower boundaries of boxes indicate the 75th and 25th percentiles; the lines within the box mark the median; the whiskers above and below boxes indicate the 90th and 10th percentiles; and cross symbols represent the means.

[Title Page](#)[Abstract](#)[Introduction](#)[Conclusions](#)[References](#)[Tables](#)[Figures](#)[◀](#)[▶](#)[◀](#)[▶](#)[Back](#)[Close](#)[Full Screen / Esc](#)[Printer-friendly Version](#)[Interactive Discussion](#)

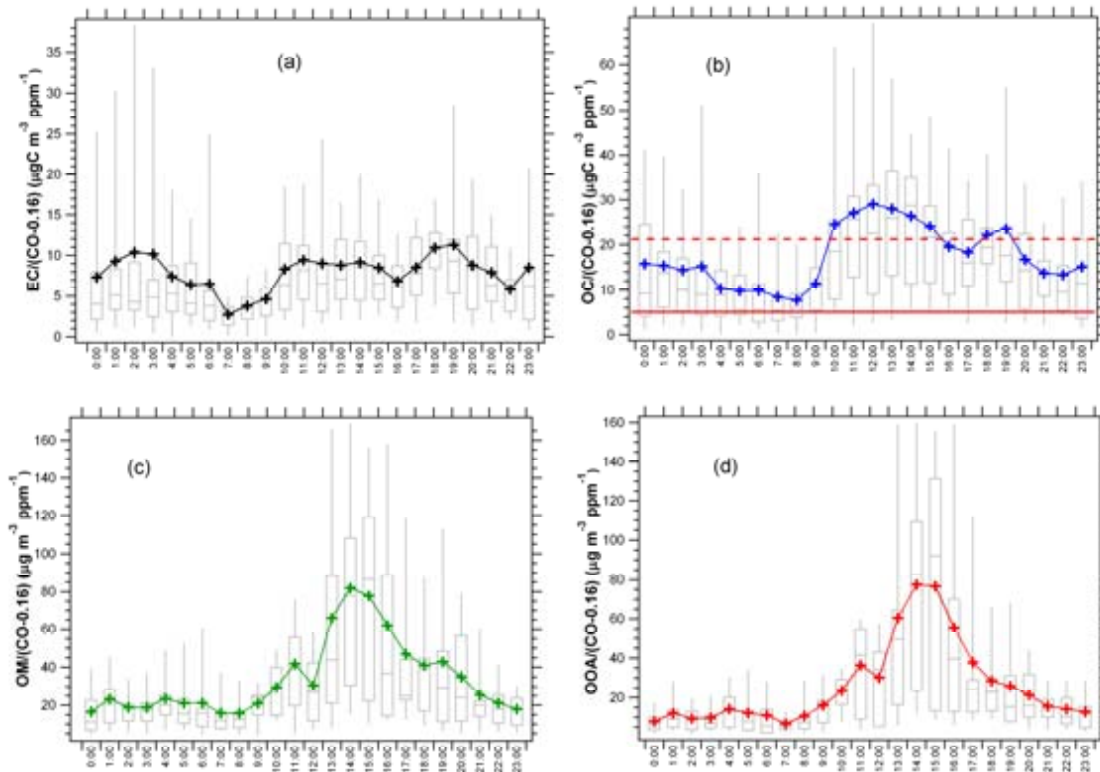


Fig. 6. Diurnal variations of different aerosol species EC (a), OC (b), OM (c), OOA (d) versus (CO-0.16). The value of 0.16 ppm was CO background concentration. The box plot is the same meaning as Fig. 5 showed. The red lines in Fig. 6b indicate estimates for the direct emissions (solid) and secondary formation after half a day of processing (dotted) of organic aerosol in the northeastern US (de Gouw et al., 2009).

Carbonaceous aerosol at a rural site of PRD

W. W. Hu et al.

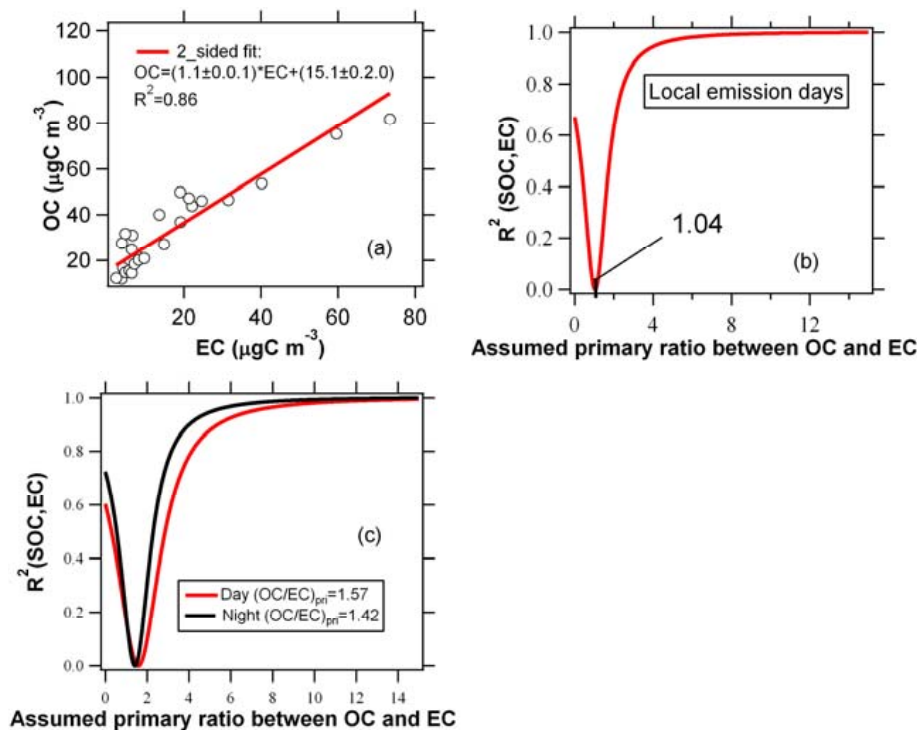


Fig. 7. (a) Scatter plot between OC and EC during the nights of local primary emission days. (b) R^2 between SOC and EC is as a function of the primary emission ratio between OC and EC in the local emission days and (c) normal days of the whole campaign.

Title Page

Abstract

Introduction

Conclusions

References

Tables

Figures

◀

▶

◀

▶

Back

Close

Full Screen / Esc

Printer-friendly Version

Interactive Discussion



Carbonaceous aerosol at a rural site of PRD

W. W. Hu et al.

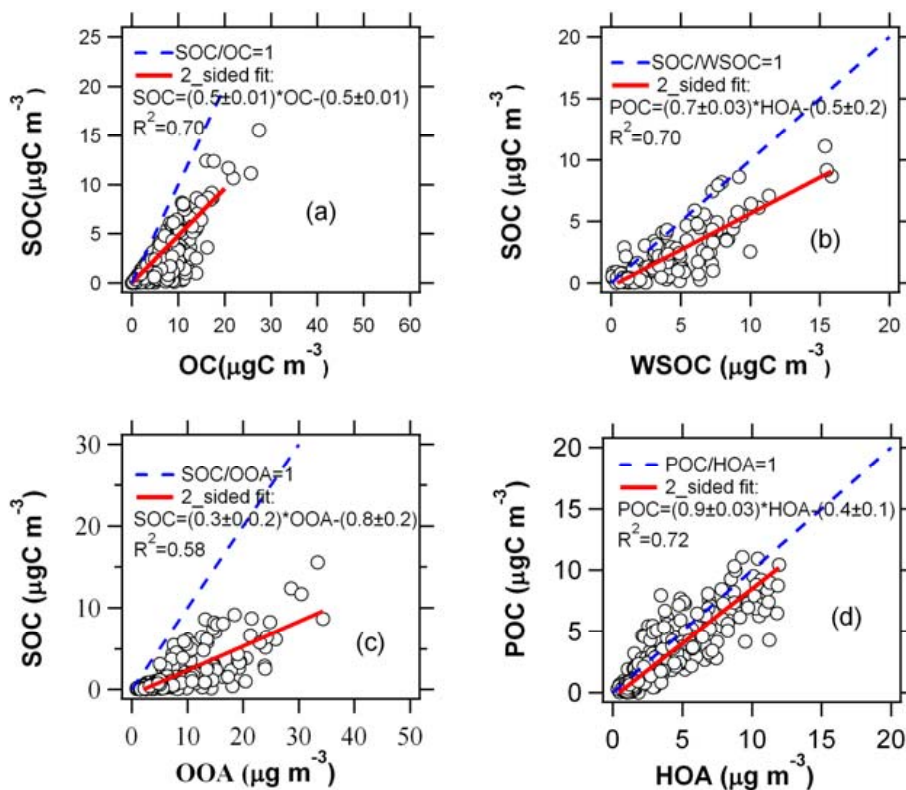


Fig. 8. Scatter plots of different organic aerosols at BG site, SOC versus OC (a), WSOC (b), OOA (c) and POC versus HOA (d).

[Title Page](#)
[Abstract](#)
[Introduction](#)
[Conclusions](#)
[References](#)
[Tables](#)
[Figures](#)
[◀](#)
[▶](#)
[◀](#)
[▶](#)
[Back](#)
[Close](#)
[Full Screen / Esc](#)
[Printer-friendly Version](#)
[Interactive Discussion](#)


**Carbonaceous
aerosol at a rural site
of PRD**

W. W. Hu et al.

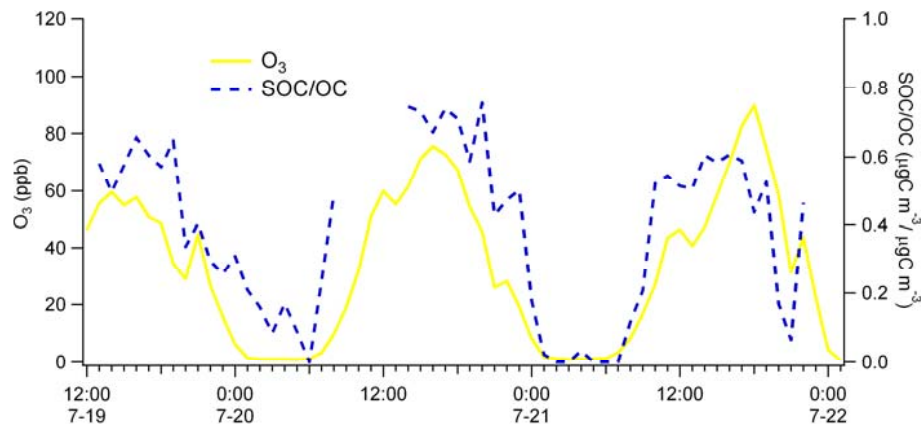


Fig. 9. The variation of SOC/OC ratio and O₃ during the photochemical active periods of 19 to 21 July 2006.

Title Page

Abstract

Introduction

Conclusions

References

Tables

Figures

◀

▶

◀

▶

Back

Close

Full Screen / Esc

Printer-friendly Version

Interactive Discussion

